INTERNAL REFLECTIONS OF AND MATCHING LAYERS FOR INTEGRATED LENS ANTENNAS

P.J.I. de Maagt, M.J.M. van der Vorst*, and M.H.A.J. Herben*
European Space Agency ESTEC, P.O. Box 299, 2200 AG Noordwijk, The Netherlands
*Eindhoven University of Technology, P.O. Box 513, 5600 MB Eindhoven, The Netherlands

Abstract

This paper deals with first-order reflected waves within and matching layers for integrated lens antennas. It appears that if the relative dielectric constant of the antenna is not too large ($\epsilon_r < 4$) the single- and double-reflected waves are sufficient to describe the process of internal reflections. Furthermore, the impact of these reflected waves on the co- and cross-polar antenna patterns is determined. For high(er) dielectric constant materials also higher-order internal reflections must be included to obtain accurate results. However, due to the rather high reflection "losses" introduced by these materials a matching layer will usually be applied. Both a quarter-wavelength matching layer and a layer with optimal thickness are described and their impact on various antenna properties is studied.

1. Introduction

A new generation of scientific instruments, included in both Earth observation and scientific missions, is under consideration at (sub)millimeter wavelengths. In the present ESA Earth observation studies, millimeter and submillimeter limbsounding instruments (e.g. MASTER and SOPRANO) are already using frequencies up to 1 THz. Also projected in this frequency band are astronomy missions (e.g. FIRST) in which the frequency range may even extend to above 3 THz. The specifications of these instruments are very stringent: very high beam efficiency, high pattern gaussicity and very low receiver noise temperature. These lead to the need for low loss, very high quality antenna patterns with low sidelobes. If the receiver is used for spacecraft applications, the requirement of robustness naturally arises. Furthermore, certain atmospheric constituents are polarised and this requires knowledge of the polarization.

As the frequency increases, it becomes more complex to manufacture the traditional waveguide based front-ends and to assemble them physically due to their small size. However, the small size can be turned into an advantage when the dimensions and tolerances required become compatible to those achieved by lithography. In this case a planar structure which integrates the antenna, mixer, local oscillator and all peripheral circuitry onto one single substrate becomes an competitive solution. Furthermore, these integrated front-ends promise advantages such as reproducibility, robustness, possible extension into an array antenna and low production costs if they are produced in high quantities.

One of the problems that has been encountered, is the fact that planar antennas on dielectric substrates couple power into substrate modes, and since these do not contribute to the primary radiation pattern, substrate mode power is generally considered as a loss mechanism. One way to overcome this problem is to simulate an infinitely thick dielectric by means of a lens. A disadvantage of all lens antenna designs is that they suffer from reflection "losses", which can affect the radiation pattern and degrade the performance of the integrated antenna. In this paper these internal reflections and the matching layers used to minimize their impact on the co- and cross-polar patterns will be treated.

2. Geometry

The general geometry of an integrated lens antenna is depicted by its two-dimensional cross-section in Figure 1. As can be seen from this figure, the antenna consists of a planar

radiating element, a dielectric slab and a lens, whose center is chosen to lie on top of the slab. It is assumed that the lens has the same dielectric constant as the slab, and that its shape is either elliptical or extended hemispherical. In order to calculate the far-field radiation patterns (co- and cross-polar) of this antenna a Geometrical Optics (GO) approach is applied inside the lens and Physical Optics (PO) outside the lens [1].

A common problem arising with these lens antennas is that the incident wave is partly reflected at the lens-air interface. The corresponding reflected power should not be treated as loss but as interference, because part of the reflected wave can leave the lens after one or more internal reflections and affect the radiation pattern.

3. Internal reflections

Figure 1 reveals three different angular domains of which domain I and III actually contribute to the field outside the dielectric lens. The first group of internal reflected rays, the so-called single-reflected rays (angular domain I), only reflect once at the surface of the lens before they contribute to the far-field radiation pattern. For rays having an angle of propagation within angular domain II it can be seen that after reflection at the lens surface they propagate directly into the substrate and there they will most likely be trapped as substrate modes. Finally, angular domain III consists of rays which will also hit the lens for a second time, but now after complete reflection at the metal plate.

Both above-mentioned internal reflected field contributions can again be treated by using a GO/PO method but to account for the divergence losses of the reflected waves a (divergence) factor has to be included, which describes the amplitude variation along a reflected ray [2]. To demonstrate the impact of the reflected waves on the antenna performance, a planar double-dipole with backing reflector will be used and the dielectric material selected is HDP or quartz with an ϵ_r of 2.31 and 4.0, respectively. The dimensions of the planar feed are: length is $0.5\lambda_d$, distance between elements is $0.4\lambda_d$ and distance between the elements and the metallic backing reflector is $0.25\lambda_d$. In order to determine the importance and the completeness of the single- and double-reflected fields, the relative powers of the different types of reflected waves have been determined and shown in Table 1 for different dielectric materials.

From Table 1 it can be seen that the reflection "losses" (P_{refl}) only slightly increase with increasing dielectric constant. The reason for this is that, although the feed patterns in the dielectric are equal, the lens illuminations are quite different for both antenna designs due to the different lens shapes. By selecting a higher dielectric constant material as quartz, the feed location shifts towards the center of the elliptical lens and this results in smaller angles of incidence and thus lower reflection coefficients at the lens surface. Furthermore, the distribution of the reflected power shows that this power is mainly contained within the single-reflected fields (P_{single}), whereas the double-reflected field contribution is negligible for both materials. Another observation that can be made is that for the two antenna designs almost the same amount of power is directly radiated into the substrate (P_{sub}). The amount of the internal reflected power that is reflected for a second time at the lens surface ($P^r_{single} + P^r_{double}$) is denoted by P_{naf} and stands for the power that is *not accounted for* in the present model. In fact this reflected power represents the higher-order internal reflected fields and in Table 1 it is shown that for the higher dielectric constant material more power is not taken into account. This means that the accuracy of the radiation patterns obtained with the inclusion of the single- and double-reflected fields is higher for HDP than for quartz (e.g. for quartz P_{naf} is 5.4%).

As an example the co- and cross-polar patterns of an elliptical lens antenna made of quartz and illuminated by a double-dipole antenna with backing reflector were calculated in the diagonal plane at 246 GHz and these normalized patterns are depicted in Figure 2. The far-field radiation patterns show that for small angles from boresight mainly the cross-polar pattern is affected by

the internal reflection contributions. However, if one observes the patterns for larger far-field angles, both the co- and cross-polar radiation patterns change significantly. Table 1 shows that by neglecting the first-order internal reflected field contributions, the beam efficiency is overestimated by more than 10%.

4. Matching layer

For the analysis of the matching layer, it is assumed that both the incident wave and the shape of the matching layer are locally plane. Then the matching layer model described in Ref. [3] can be used, resulting in a reflection and transmission coefficient for the matching layer which accounts for an infinite number of internal reflections (see Figure 3). These "infinite" reflection coefficients are given by:

$$R_\infty = R_1 + T_1 T_3 R_2 P_d^2 P_a \sum_{m=0}^{\infty} (R_2 R_3 P_d^2 P_a)^m = R_1 + \frac{T_1 T_3 R_2 P_d^2 P_a}{1 + R_2 R_1 P_d^2 P_a} \tag{1.a}$$

$$T_\infty = T_1 T_2 P_d \sum_{m=0}^{\infty} (R_2 R_3 P_d^2 P_a)^m = \frac{T_1 T_2 P_d}{1 + R_2 R_1 P_d^2 P_a} \tag{1.b}$$

where subscript 1 indicates the lens to matching layer interface, subscript 2 the matching layer to free space interface and subscript 3 indicates the matching layer to lens interface. In these equations two phase terms are introduced, of which P_d describes the phase shift that results from the propagation of a ray through the matching layer and P_a describes the phase shift that is due to the path length difference between subsequent rays in a far-field observation point, which is caused by the fact that the rays leave the slab at different points (see Figure 3). Equation (1) can be used for both perpendicular and parallel polarization, if the appropriate Fresnel reflection and transmission coefficients are substituted.

The choice of a quarter-wavelength matching layer ($\epsilon_m = \sqrt{\epsilon_d \epsilon_0}$) will result in a zero reflection field in case of a normal incident wave at the lens-matching layer boundary. However, with oblique incidence, the quarter-wavelength layer does not reduce the reflections completely and an optimal thickness of the matching layer must be determined.

It should be noted that the phase of the 'infinite' transmission coefficient changes at the lens surface because the angle of incidence changes, and therefore the matching layer can still affect the antenna parameters such as the gaussian beam efficiency and the polarization efficiency.

In defining the optimal matching layer for a specific lens antenna design, it is important to determine first its thickness (d_{opt}) as a function of the angle of incidence, at which the 'infinite' transmission coefficient is maximal. By substitution of $P_d^2 P_a = \exp(-j\xi)$ in Equation 1.b and by taking the derivative of $|T_\infty|$ with respect to ξ, the maximum of the 'infinite' transmission coefficient is found for $\xi = -\pi$, resulting in an optimal thickness profile of the matching layer given by:

$$\frac{d_{opt}}{\lambda_m} = \frac{1}{4\cos\theta^{tl}} = \frac{1}{\sqrt{1 - n_d \sin^2\theta^i}} \tag{2}$$

This equation holds for both perpendicular and parallel polarization. Furthermore, it appears that for this optimal matching layer design the 'infinite' reflection and transmission coefficients for both perpendicular (per.) and parallel (par.) polarization are equal as can be seen from Figure 4.

To determine the influence of the matching layer three configurations will be compared: no matching layer (n.m.l.), a quarter-wavelength matching layer (q.m.l.) and a layer with the optimal thickness profile given by Equation 2 (o.m.l.). Two planar feeds will be used, both with either a silicon or quartz elliptical shaped lens. The diameter and the operating frequency are chosen as

15.0 mm and 246 GHz, respectively. In the first example a silicon lens is used, which is illuminated by the same double-dipole feed as used in the previous section. Both the co- and cross-polar radiation pattern are calculated and depicted in Figure 5. Secondly, a double-slot feed antenna (length is $0.28\lambda_0$ and distance between elements is $0.16\lambda_0$) on a silicon dielectric lens is used and the resulting co- and cross-polar radiation pattern are also shown in Figure 5. Comparing the radiation patterns of the integrated lens antennas with and without a matching layer, reveals that both the directivity and the sidelobe levels are increased when a matching layer is applied, but that the shape of the co-polar patterns does not seem to change dramatically. The cross-polar patterns however are affected significantly. In case of the double-dipole feed with backing reflector the cross-polar level increases while for the antenna with the double-slot feed it decreases. The explanation for this is the different polarization dependencies of the ('infinite') transmission coefficients for the three matching layer designs. For example, the transmission coefficient of the optimal matching layer is polarization independent, while for the other layers it does depend on polarization as shown in figure 4.

Next, also some other important antenna parameters are determined and shown in Table 2 for a double-slot (with a length of $0.28\lambda_0$ and a distance between elements of $0.2\lambda_0$) on quartz. It can be seen that the quarter-wavelength matching layer and the optimal matching layer show comparable performances. It is clear from the table that the quartz lens designs have the lowest spillover efficiency (η_s), beam efficiency (η_b) and gaussian beam efficiency (η_g). Furthermore, Table 2 reveals that the transmission efficiency (η_{tr}) can be improved by more than 10% for the quartz designs and by even more than 25% for the silicon designs and that also the gaussian beam efficiency is improved by the use of a matching layer.

5. Conclusions

Comparing the radiation patterns of the integrated lens antennas with and without the inclusion of internal reflections, reveals that in case of elliptical lenses the differences found in the main lobe and the first few sidelobes of the co-polar patterns are negligible. Only for larger angles from boresight the influence of the internal reflections on the co-polar patterns becomes significant. By neglecting the first-order internal reflected field contributions, the beam efficiency can be overestimated by more than 10%. For the cross-polar patterns it has become clear that the internal reflected rays can have a major effect on both the shape and level of the cross-polar radiation patterns.

It has been shown that for integrated lens antennas with a low dielectric constant ($\epsilon_r < 4$) the first-order internal reflected fields are sufficient to determine the influence of the reflected fields on the antenna performance.

Furthermore, it was also found that the use of a matching layer for high dielectric constant lenses reduces the reflection "losses" by more than 10%. Also the Gaussian beam efficiency can be improved considerably. The impact of the matching layer on the cross-polar levels depends on both the lens material and the feed element used.

References

[1] Filipovic, D.F., S.S. Gearhart and G.M. Rebeiz, "*Double-slot antennas on extended hemispherical and elliptical silicon dielectric lenses*", IEEE Trans. on Microwave Theory and Tech., vol 41, no. 10, pp. 1738-1749, 1993.

[2] Lee, S. W. et al., "*Refraction at a curved dielectric interface: Geometrical Optics solution*", IEEE Trans. on Microwave Theory and Tech., vol. 30, no. 1, pp. 12-19, 1982.

[3] van Houten, J. M., and M.H.A.J. Herben, "*Analysis of a phase-correcting Fresnel-zone plate antenna with dielectric/transparent zones*", Journal of Electromagnetic Waves and Applications, vol. 8, no. 7, pp. 847-858, 1994.

Table 1 : Power distribution of an elliptical lens illuminated by a double-dipole feed with backing reflector. All power values are given in percentages of the total power incident to the lens.

ϵ_r	P_{trans}	P_{refl}	P_{single}	P_{double}	P_{sub}	P^t_{single}	P^r_{single}	P^t_{double}	P^r_{double}	P_{naf}
2.31	76.9	23.1	18.9	0.0	4.2	17.4	1.5	0.0	0.0	1.5
4.00	76.8	23.2	19.1	0.2	3.9	13.8	5.3	0.1	0.1	5.4

Table 2 : Efficiencies and relative first sidelobe levels of an elliptical 15.0 mm lens, illuminated by a planar feed at 246 GHz.

| feed antenna	matching layer	ϵ_r	sidelobe level(dB)	η_s (%)	η_{tr} (%)	η_{beam} (%)	η_{gaus} (%)
d.dipole	no	11.7	-18.6	99.9	65.6	87.8	85.6
d.dipole	constant	11.7	-18.9	99.9	93.7	88.8	86.4
d.dipole	optimal	11.7	-18.4	99.9	94.8	87.5	85.9
d.dipole	no	4.00	-17.0	94.2	77.3	80.7	78.5
d.dipole	constant	4.00	-16.7	94.2	89.5	81.8	81.5
d.dipole	optimal	4.00	-14.4	94.2	91.9	72.2	81.7
d.slot	no	11.7	-23.0	91.1	70.4	90.7	87.8
d.slot	constant	11.7	-22.4	91.1	96.0	88.8	90.7
d.slot	optimal	11.7	-21.8	91.1	96.6	87.8	90.9
d.slot	no	4.00	-16.9	65.1	78.7	73.2	73.1
d.slot	constant	4.00	-16.4	65.1	87.7	72.9	81.2
d.slot	optimal	4.00	-14.1	65.1	89.3	66.2	81.6
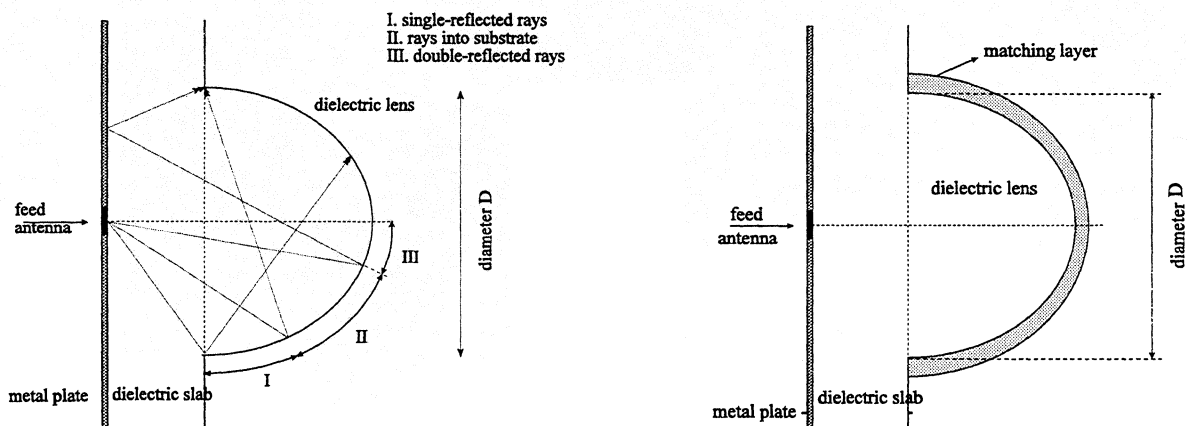
**Figure 1** Antenna geometry; left: internal reflections, right: matching layer.
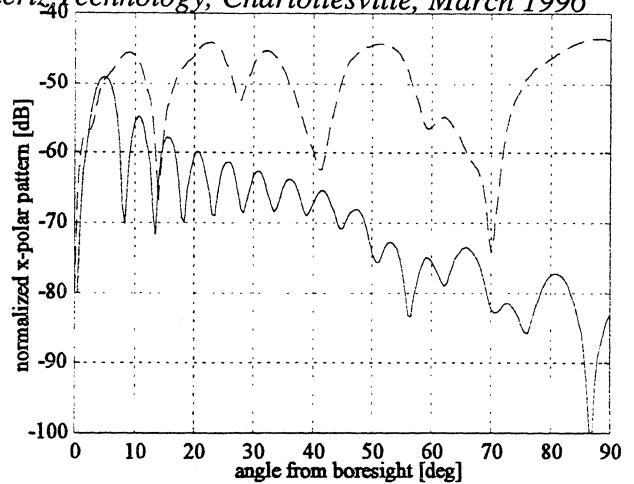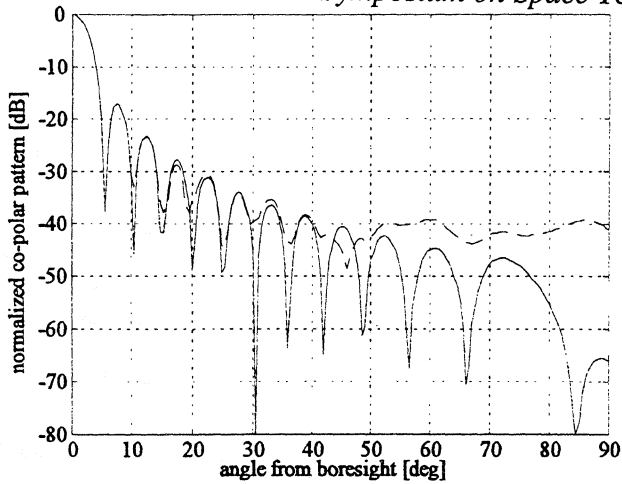
Figure 2 Normalized co-and cross-polar patterns, in the diagonal plane at 246 GHz, of a 15mm diameter elliptical quartz lens antenna illuminated by a double dipole with backing reflector (solid curve: without internal reflections, dashed: with internal reflections).
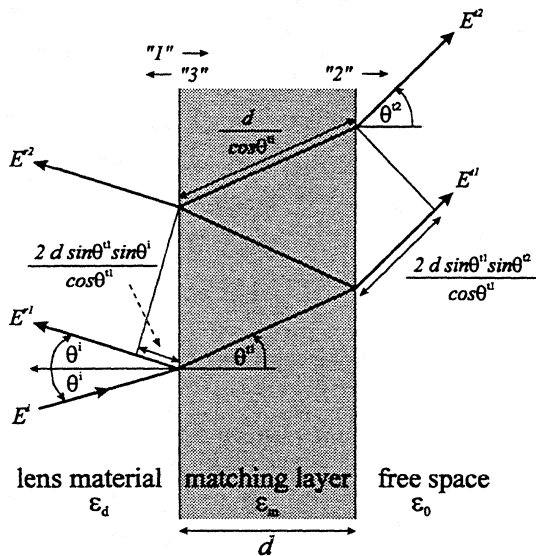
Figure 3 Ray tracing of a plane wave through a lossless dielectric matching layer.
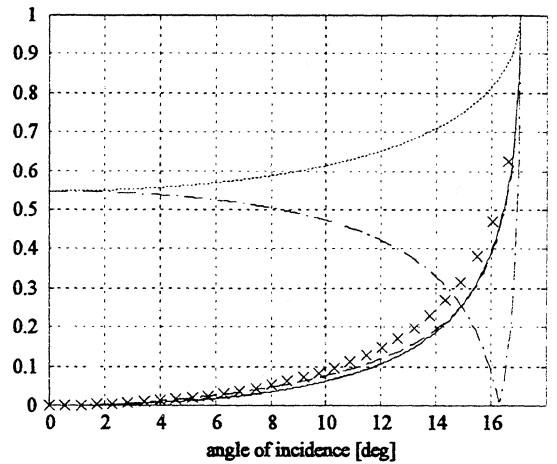
Figure 4 Magnitude of reflection coefficients for a silicon substrate (solid: o.m.l., dashed: q.m.l.par., cross: q.m.l.per., dashdotted: n.m.par., and dotted: n.m.per.)
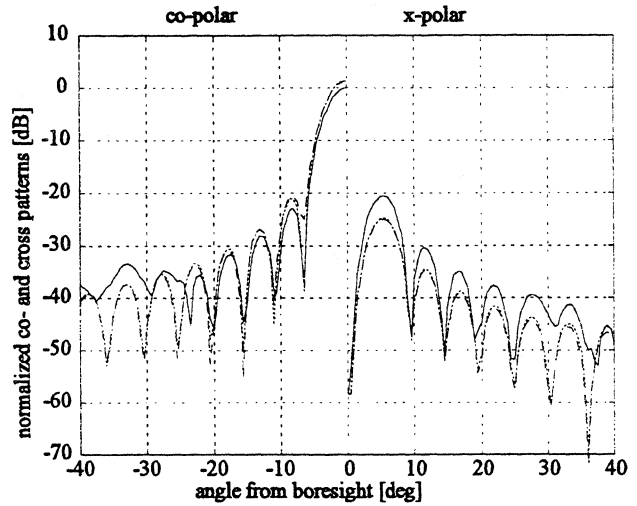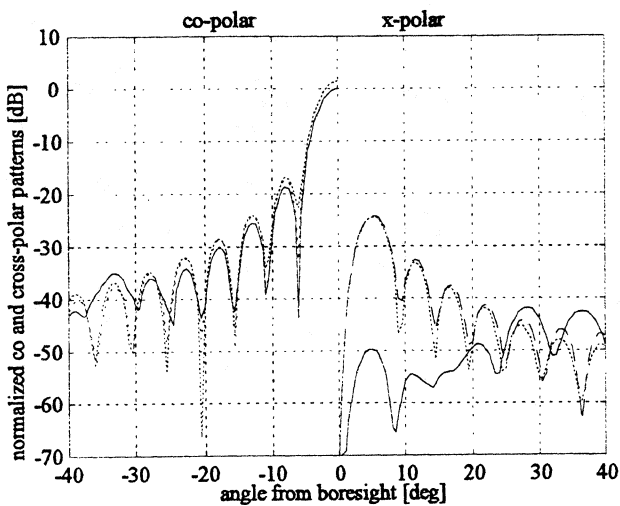
Figure 5 Normalized co- and cross-polar patterns, in the diagonal plane at 246 GHz, of a 15 0mm diameter silicon lens antenna (solid curve: without matching layer, dashed curve: with constant thickness matching layer, dotted: optimal thickness matching layer)
left: double dipole with backing reflector   right: double slot.